

Alternative method for measuring both the refractive indices and the thickness of silver-halide holographic plates

Cheng-Chih Hsu

Industrial Technology Research Institute
Center for Measurement Standards
Building 16, 321 Kuang Fu Road,
Section 2
Hsin-Chu 30050, Taiwan

Jiun-You Lin

National Chiao Tung University
Institute of Electro-Optical Engineering
1001 Ta-Hsueh Road
Hsin-Chu 30050, Taiwan

Kun-Huang Chen

Feng Chia University
Department of Electrical Engineering
100 Wenhwa Road
Seatwen, Taichung 40724
Taiwan

Der-Chin Su, MEMBER SPIE

National Chiao Tung University
Institute of Electro-Optical Engineering
1001 Ta-Hsueh Road
Hsin-Chu 30050, Taiwan

1 Introduction

Silver-halide holographic plates^{1,2} are widely used because of their high sensitivity and commercial availability. According to the coupled wave theory,³ their thickness and refractive indices strongly influence the characteristics of holograms. To enhance the quality of a hologram, it is very important to measure accurately the associated thickness and refractive indices of a holographic plate.² There are several methods⁴⁻¹⁰ proposed for measuring the refractive index of material, but they are suitable only for either absorbing materials⁴⁻⁷ or nonabsorbing materials.⁸⁻¹⁰ Although some other methods¹¹⁻¹³ are also proposed for measuring the thickness, they are applied only for the thickness being smaller than the light wavelength. However, the commercial silver-halide holographic plates consist of a weak-absorbing emulsion layer and a nonabsorbing substrate, and their thicknesses are far larger than the light wavelength. To our knowledge, there is no method for measuring both the refractive indices and the thickness of a thick weak-absorbing material and its substrate with single optical configuration. In this work, an alternative method for achieving all these measurements in one setup is presented. This method is based on Fresnel's equations,¹⁴ heterodyne interferometry,¹⁵ and multiwavelength interferometry.¹⁶ Three pieces of holographic plates are measured, and the measured results are in good correspondence with the reference data. The validities of this method are demonstrated.

Abstract. First, the phase differences between *s*- and *p*-polarizations of a circularly polarized heterodyne light beam reflected from the emulsion layer, and that from its substrate, are measured, respectively. The measured data are substituted into specially derived equations, so the refractive indices of the emulsion layer and its substrate can be calculated. Second, the variations of phase differences between *s*- and *p*-polarizations due to the wavelength shifts and the extraction of the holographic plate in a modified Michelson interferometer are measured. Then, the thickness of the emulsion layer and its substrate can be estimated based on the measured values of refractive indices, the wavelength shifts, and the phase difference variations. This method has some advantages, such as high resolution and easy operation in only one optical configuration. © 2005 Society of Photo-Optical Instrumentation Engineers. [DOI: 10.1117/1.1902624]

Subject terms: silver-halide holographic; refractive index; heterodyne interferometry.

Paper 040282R received May 17, 2004; revised manuscript received Nov. 16, 2004; accepted Nov. 17, 2004; published online May 23, 2005.

2 Principle

The schematic diagram of this method is shown in Fig. 1. For convenience, the $+z$ axis is chosen to be along the light propagation direction and the x axis is along the direction perpendicular to the paper plane. A light coming from a heterodyne light source¹⁷ has an angular frequency difference ω between *s*- and *p*-polarizations, and its Jones vector¹⁸ can be written as

$$E = \frac{1}{\sqrt{2}} \begin{bmatrix} \exp(i\omega t/2) \\ \exp(-i\omega t/2) \end{bmatrix}. \quad (1)$$

It is incident on a beamsplitter (BS) and is divided into two parts: the transmitted light and the reflected light. The transmitted light is used to measure the refractive indices of both the emulsion layer and its substrate, and the reflected light is for measuring the thickness. The details are described as follows.

2.1 Refractive Index Measurements

The transmitted light passes through a quarter-wave plate Q with the fast axis at 0 deg to the x axis. The Jones vector of the light can be written as¹⁹

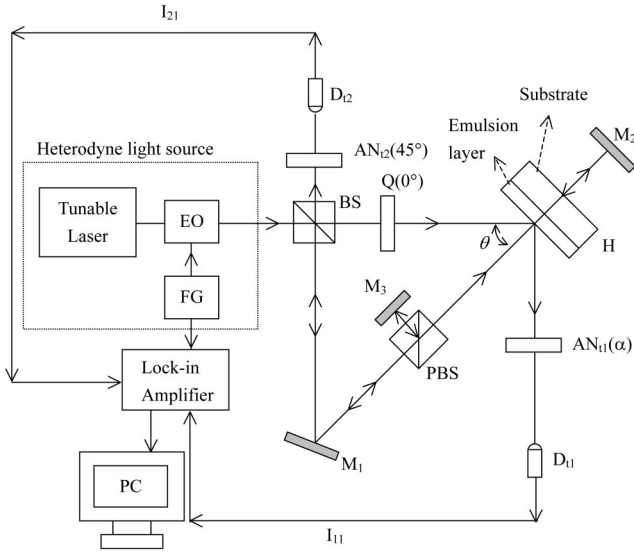


Fig. 1 Schematic diagram for measuring the phase differences.

$$E_i = Q(0 \text{ deg}) \cdot E = \begin{bmatrix} \cos\left(\frac{\omega t}{2}\right) \\ -\sin\left(\frac{\omega t}{2}\right) \end{bmatrix}$$

$$= \frac{1}{2} \begin{pmatrix} 1 \\ i \end{pmatrix} \exp\left(i \frac{\omega t}{2}\right) + \frac{1}{2} \begin{pmatrix} 1 \\ -i \end{pmatrix} \exp\left(-i \frac{\omega t}{2}\right). \quad (2)$$

From Eq. (2), we can see that the right- and left-circular polarizations have angular frequency shifts $\omega/2$ and $-\omega/2$, respectively. Thus, there is an angular frequency difference ω between them. This circularly polarized heterodyne light beam is incident at θ onto the silver-halide emulsion layer. Then the reflected light passes through an analyzer AN_{t1} with the transmission axis at α to the x axis, and enters a photodetector D_{t1} . Hence, the intensity detected by D_{t1} can be expressed as

$$I_{11} = I_0 [1 + \gamma \cos(\omega t + \phi_1)], \quad (3)$$

where I_0 and γ are the bias intensity and the visibility of the signal, and ϕ_1 is the phase difference between the p - and s -polarizations coming from the reflection of the emulsion layer. They can be written as

$$I_0 = \frac{1}{2} (|r_p|^2 \cos^2 \alpha + |r_s|^2 \sin^2 \alpha), \quad (4)$$

$$\gamma = \frac{\sqrt{A^2 + B^2}}{I_0}, \quad (5)$$

$$A = \frac{1}{2} (|r_p|^2 \cos^2 \alpha - |r_s|^2 \sin^2 \alpha), \quad (6)$$

$$B = \frac{1}{2} (r_p r_s^* + r_s r_p^*) \sin \alpha \cos \alpha, \quad (7)$$

and

$$\phi_1 = \tan^{-1} \left(\frac{B}{A} \right) = \tan^{-1} \left[\frac{(r_p r_s^* + r_s r_p^*) \sin \alpha \cos \alpha}{|r_p|^2 \cos^2 \alpha - |r_s|^2 \sin^2 \alpha} \right], \quad (8)$$

where r_p , r_s , r_p^* , and r_s^* are the reflection coefficients and its conjugates of p - and s -polarizations, respectively. According to the Fresnel's equations, we have¹⁴

$$r_p = \frac{\cos[\sin^{-1}(\sin \theta/n_e)] - n_e \cos \theta}{\cos[\sin^{-1}(\sin \theta/n_e)] + n_e \cos \theta}, \quad (9)$$

and

$$r_s = \frac{\cos \theta - n_e \cos[\sin^{-1}(\sin \theta/n_e)]}{\cos \theta + n_e \cos[\sin^{-1}(\sin \theta/n_e)]}, \quad (10)$$

where n_e is the refractive index of the silver-halide emulsion layer and it can be written as $n_e = n + ik$.

On the other hand, the modulated electronic signal of the heterodyne light source is filtered and becomes the reference signal. It has the form of

$$I_r = \frac{1}{2} [1 + \cos(\omega t)]. \quad (11)$$

Both these two sinusoidal signals I_{11} and I_r are sent to a lock-in amplifier and their phase difference ϕ_1 can be measured accurately.

From Eqs. (8), (9), and (10), it is obvious that the phase difference ϕ_1 is a function of n , k , and α , and it can be experimentally measured for each given α . To evaluate the values of n and k , we require two phase differences ϕ_{11} and ϕ_{12} that correspond to two azimuth angles α_1 and α_2 , respectively. Hence, a set of simultaneous equations

$$\phi_{11} = f(n, k, \alpha_1), \quad (12)$$

$$\phi_{12} = f(n, k, \alpha_2), \quad (13)$$

are obtained. If these simultaneous equations are solved, then the refractive indices n and k of the emulsion layer can be estimated.

Second, let the tested holographic plate be rotated by

$$\phi_{13} = \tan^{-1} \left\{ \frac{[1 + 2n_s^2 + 2(n_s^2 - 1)\cos 2\theta + \cos 4\theta]\sin 4\alpha_3 - 8n_s \cos \theta \sin^2 \theta \sin 2\alpha_3 \left(\frac{4n_s^2 - 2 + 2\cos 2\theta}{n_s^2}\right)^{1/2}}{4[n_s^2 - 1 + (1 + n_s^2)\cos 2\theta]} \right\}, \quad (14)$$

where n_s is the refractive index of the substrate. Because the substrate is a nonabsorbing material, its refractive index can be solved from Eq. (14) only given an azimuth angle α_3 of AN_{t1} and the measured value of ϕ_{13} .

2.2 Thickness Measurements

As shown in Fig. 1, the reflected light coming from the BS is reflected again by a mirror M_1 and enters a modified Michelson interferometer. It consists of a polarization beamsplitter (PBS), two mirrors M_2 and M_3 , an analyzer AN_{t2} , and a photodetector D_{t2} . The tested holographic plate H is located in one arm and the light beam passes through this plate perpendicularly. In the interferometer, PBS divides the light into two beams. The paths of these two beams are: 1. $PBS \rightarrow M_3 \rightarrow PBS \rightarrow M_1 \rightarrow BS \rightarrow AN_{t2} \rightarrow D_{t2}$ (for the reflected s -polarization light), and 2. $PBS \rightarrow H \rightarrow M_2 \rightarrow PBS \rightarrow M_1 \rightarrow BS \rightarrow AN_{t2} \rightarrow D_{t2}$ (for the transmitted p -polarization light). If the transmission axis of AN_{t2} is 45 deg to the x axis, then Jones vectors of p - and s -polarizations arriving at D_{t2} are

$$E_p = \frac{1}{2\sqrt{2}} \begin{pmatrix} 1 \\ 1 \end{pmatrix} \exp\left[i\left(\frac{\omega t}{2} + \phi_{21}\right)\right] \exp\left(-\frac{4\pi k_1 d_e}{\lambda_1}\right), \quad (15)$$

and

$$E_s = \frac{1}{2\sqrt{2}} \begin{pmatrix} 1 \\ 1 \end{pmatrix} \exp\left[i\left(-\frac{\omega t}{2}\right)\right], \quad (16)$$

where k_1 is the imaginary index of the emulsion layer at wavelength λ_1 , d_e is the thickness of the emulsion layer, and d_s is that of the substrate, respectively. ϕ_{21} is the phase difference due to the optical path difference between the two arms, and it can be expressed as

$$\phi_{21} = \frac{4\pi[n_1 d_e + n_{s1} d_s + d]}{\lambda_1}, \quad (17)$$

where n_1 and n_{s1} are the real index of the emulsion layer and the refractive index of the substrate at wavelength λ_1 , and d is the path difference between the two arms, except for the thickness of the tested holographic plate in the interferometer, respectively. Hence, the intensity of the test signal received by D_{t2} can be expressed as

180 deg such that the light beam is incident at identical incident angle θ on its substrate, then the test signal has a similar mathematical form of Eq. (3) but with a different phase difference ϕ_{13} . It can be expressed as

$$I_{21} = |E_p + E_s|^2 = \frac{1}{4} \left[1 + \exp\left(-\frac{8\pi k_1 d_e}{\lambda_1}\right) + 2 \exp\left(-\frac{4\pi k_1 d_e}{\lambda_1}\right) \cos(\omega t + \phi_{21}) \right]. \quad (18)$$

When the wavelength of the heterodyne light source is slightly shifted to λ_2 , then it becomes

$$I_{22} = |E'_p + E'_s|^2 = \frac{1}{4} \left[1 + \exp\left(-\frac{8\pi k_2 d_e}{\lambda_2}\right) + 2 \exp\left(-\frac{4\pi k_2 d_e}{\lambda_2}\right) \cos(\omega t + \phi_{22}) \right], \quad (19)$$

where k_2 is the imaginary index of the emulsion layer at wavelength λ_2 . These sinusoidal signals I_{21} , I_{22} , and I_r are sent to the lock-in amplifier, then ϕ_{21} and ϕ_{22} can be obtained. Hence, the variations of phase difference $\Delta\phi$ due to the wavelength shift $\Delta\lambda_1 (= \lambda_2 - \lambda_1)$ can be derived and written as

$$\begin{aligned} \Delta\phi &= \phi_{22} - \phi_{21} \\ &= \frac{4\pi[d_e(n_2\lambda_1 - n_1\lambda_2) + d_s(n_{s2}\lambda_1 - n_{s1}\lambda_2) - d\Delta\lambda_1]}{\lambda_1\lambda_2}, \end{aligned} \quad (20)$$

where n_2 and n_{s2} are the real index of the emulsion layer and the refractive index of the substrate at wavelength λ_2 , respectively.

Then, remove the tested holographic plate H from the interferometer, and the phase differences are measured similarly. We also obtain ϕ_{31} at λ_1 , and ϕ_{32} at λ_2 . So the phase difference variation $\Delta\phi'$ between two measurements can be written as

$$\Delta\phi' = \phi_{32} - \phi_{31} = -\frac{4\pi(d_e + d_s + d)\Delta\lambda_1}{\lambda_1\lambda_2}. \quad (21)$$

Consequently, we have

$$\Psi = \Delta \phi' - \Delta \phi = \frac{4\pi[d_e(n_1\lambda_2 - n_2\lambda_1 - \Delta\lambda_1) + d_s(n_{s1}\lambda_2 - n_{s2}\lambda_1 - \Delta\lambda_1)]}{\lambda_1\lambda_2} \tag{22}$$

Because $|\Delta\lambda|$ is so small, we have $n_1 \cong n_2 \cong n$ and $n_{s1} \cong n_{s2} \cong n_s$. Then Eq. (22) can be rewritten as

$$\Psi = \frac{4\pi[(n-1)d_e + (n_s-1)d_s]\Delta\lambda_1}{\lambda_1\lambda_2} \tag{23}$$

From Eq. (23), it is obvious that Ψ is a function of d_e , d_s , and $\Delta\lambda$. Hence, to evaluate the values of d_e and d_s , we require two phase differences Ψ_1 and Ψ_2 that correspond to the wavelength shifts $\Delta\lambda_1 = \lambda_2 - \lambda_1$ and $\Delta\lambda_2 = \lambda_3 - \lambda_1$. Hence, a set of simultaneous equations

$$\Psi_1 = f(d_e, d_s, \lambda_1, \lambda_2, \Delta\lambda_1), \tag{24}$$

$$\Psi_2 = f(d_e, d_s, \lambda_1, \lambda_3, \Delta\lambda_2), \tag{25}$$

are obtained. If these simultaneous equations are solved, then the thickness d_e and d_s can be estimated.

3 Experiments and Results

To show the feasibility of this method, we measured the refractive indices and the thickness of two Slavich holographic plates (PFG-01 and VRP-M) and a hologram fabricated with a VRP-M holographic plate at 25°C. The heterodyne light source consisting of a tunable diode laser (Model 6304, New Focus) and an electro-optic modulator (EO) driven by a function generator (FG) was used, as shown in Fig. 1. The frequency of the sawtooth signal applied to the EO was 1 kHz. A lock-in amplifier with resolution 0.001 deg (Model SR850, Stanford Research System) was used to measure the phase difference, and a personal computer was employed to record and analyze the data. For convenience, the experimental conditions $\theta = 59$ deg, $\alpha_1 = 40$ deg, $\alpha_2 = 60$ deg, $\alpha_3 = 45$ deg, $\lambda_1 = 632.8$ nm, $\lambda_2 = 632.79$ nm, $\lambda_3 = 632.81$ nm, $\Delta\lambda_1 = -0.01$ nm, and $\Delta\lambda_2 = 0.01$ nm were used. The measurement and estimated results are summarized in Tables 1 and 2. The reference data from Refs. 2 and 7 and the measured values of the plate thickness with a conventional micrometer are listed in Table 3 for comparison. It is clear that they show good agreement.

Table 1 Measurement results. Note that VRPM* means the hologram fabricated with a VRPM holographic plate.

Phase difference (in deg.)	PFG-01	VRPM	VRPM*
ϕ_{11}	1.957	2.056	-0.05
ϕ_{12}	0.945	0.995	-0.03
ϕ_{13}	5.247	5.038	4.833
Ψ_1	23.252	23.085	23.161
Ψ_2	-23.252	-23.086	-23.162

In the prior experiments, we showed that the values of n and k could be evaluated by measuring two phase differences ϕ_{11} and ϕ_{12} that correspond to two azimuth angles α_1 and α_2 , respectively. To evaluate the values of n and k more accurately, the relations between ϕ_1 and α were also measured under the conditions $\theta = 59$ deg and $\lambda_1 = 632.8$ nm. The measured results and the associated fitting curves are shown in Fig. 2. Then, based on these fitting curves, n and k can be evaluated with Eqs. (4) through (8) and by the least-square method. For comparison, these evaluated values of n and k are also listed into Table 2 with superscript #. Theoretically, they are more accurate than the results obtained with two phase differences ϕ_{11} and ϕ_{12} . The differences between these two results are small.

4 Discussions

From Eqs. (8), (14), and (23), we get

$$|\Delta n| = \frac{-B_2|\Delta\phi_{11}| + B_1|\Delta\phi_{12}|}{A_1B_2 - A_2B_1}, \tag{26}$$

$$|\Delta k| = \frac{-A_2|\Delta\phi_{11}| + A_1|\Delta\phi_{12}|}{A_2B_1 - A_1B_2}, \tag{27}$$

$$|\Delta n_s| = \frac{|\Delta\phi_{13}|}{C_1}, \tag{28}$$

$$|\Delta d_e| = \frac{\lambda_1\lambda_2|\Delta\Psi|}{4\pi(n_e-1)|\Delta\lambda_1|} = \frac{|\Delta\Psi|\Lambda_{eq}}{4\pi(n_e-1)}, \tag{29}$$

and

$$|\Delta d_s| = \frac{\lambda_1\lambda_2|\Delta\Psi|}{4\pi(n_s-1)|\Delta\lambda_1|} = \frac{|\Delta\Psi|\Lambda_{eq}}{4\pi(n_s-1)}, \tag{30}$$

where

$$A_1 = \left| \frac{\partial\phi_{11}}{\partial n} \right|, \quad A_2 = \left| \frac{\partial\phi_{12}}{\partial n} \right|, \quad B_1 = \left| \frac{\partial\phi_{11}}{\partial k} \right|,$$

Table 2 Estimated results. Note that superscript # represents the estimated values with the fitting curves of ϕ_1 versus α shown in Fig. 4, Eq. (8), and the least-square method.

Parameter	PFG-01	VRPM	VRPM*
n	1.60923	1.60626	1.66591
	1.60875 [#]	1.60544 [#]	1.66513 [#]
k	0.000071	0.000043	0.004866
	0.000075 [#]	0.000039 [#]	0.00541 [#]
n_s	1.51508	1.51508	1.51508
d_e (μm)	7.32	5.69	5.35
d_s (mm)	2.502	2.486	2.494

Table 3 Reference data. Note that superscripts a, b, and c represent the reference data coming from Refs. 7 and 2, and Scott Limited, and superscript d represents the measured values with a conventional micrometer, respectively.

Parameter	PFG-01	VRPM	VRPM*
n	1.609 ^a	1.604 ^b	1.665 ^b
k	0.00008 ^a	0.00004	0.00536
n_s	1.51509 ^c	1.51509 ^c	1.51509 ^c
d_e (μm)	7.31 ^a	5.7 ^b	5.35 ^b
d_s (mm)	2.51 ^d	2.50 ^d	2.50 ^d

$$B_2 = \left| \frac{\partial \phi_{12}}{\partial k} \right|, \quad C_1 = \left| \frac{\partial \phi_{13}}{\partial n_s} \right|, \quad (31)$$

and $|\Delta n|$, $|\Delta k|$, $|\Delta n_s|$, $|\Delta d_e|$, $|\Delta d_s|$, $|\Delta \phi_{11}|$, $|\Delta \phi_{12}|$, $|\Delta \phi_{13}|$, and $|\Delta \Psi|$ are the errors of n , k , n_s , d_e , d_s , ϕ_{11} , ϕ_{12} , ϕ_{13} , and Ψ , respectively. Λ_{eq} is the equivalent wavelength ($\cong 40$ nm in our experiments). The angular resolution of the lock-in amplifier, second harmonic error, and polarization-mixing errors are the factors that influence the accuracy of the phase difference in this method. According to Chiu, Lee, and Su's calculations,²⁰ the total phase difference errors of $|\Delta \phi_{11}|$, $|\Delta \phi_{12}|$, $|\Delta \phi_{13}|$, and $|\Delta \Psi|$ can be decreased to 0.03 deg. Substituting the conditions $|\Delta \phi_{11}| = |\Delta \phi_{12}| = |\Delta \phi_{13}| = |\Delta \Psi| = 0.03$ deg, $\lambda_1 = 632.8$ nm, $\lambda_2 = 632.79$ nm, $\Delta \lambda_1 = -0.01$ nm, and the measurement results of n_e and n_s into Eqs. (26) through (31), the measurement errors of each plate can be calculated with the software MATHEMATICA. The results are summarized in Table 4.

According to Chiu, Lee, and Su,²⁰ we understand that the phase difference error depends on the phase difference, and it becomes very small as the phase difference approaches zero. Substituting our experimental conditions into Eqs. (4) and (8), the curves of ϕ_1 and γ versus α for some different θ can be plotted in Figs. 3(a) and 3(b), re-

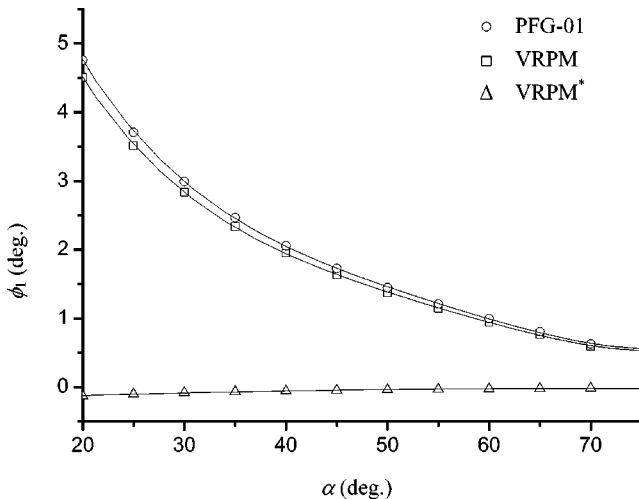


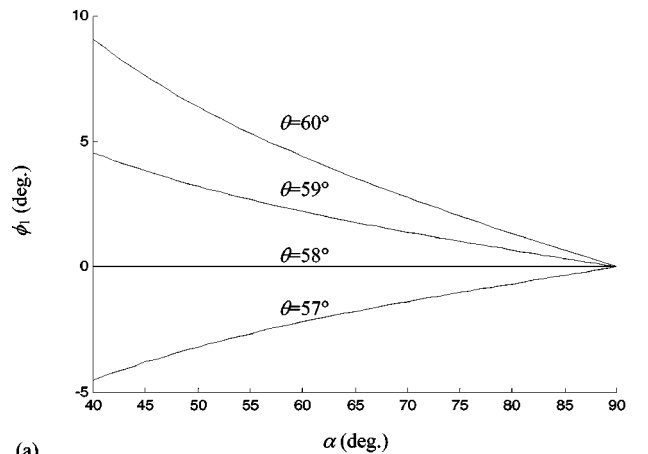
Fig. 2 Measured data between ϕ_1 and α , and the associated fitting curves.

Table 4 Estimated errors of Δn , Δk , Δn_s , Δd_e , and Δd_s .

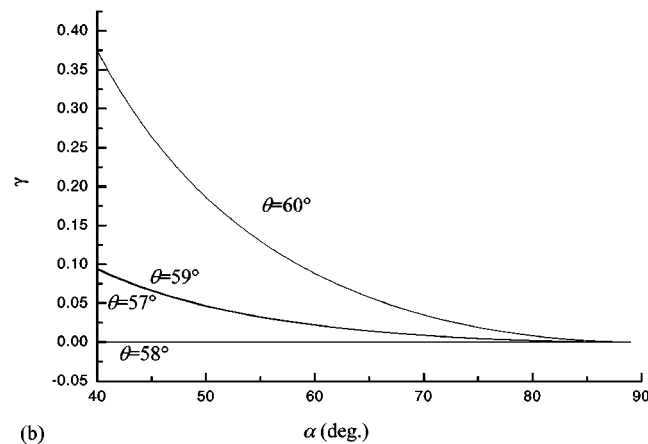
Parameter error	PFG-01	VRP-M	VRP-M*
$ \Delta n $	2.28×10^{-5}	3.48×10^{-5}	1.07×10^{-5}
$ \Delta k $	2.41×10^{-6}	2.70×10^{-6}	2.33×10^{-6}
$ \Delta n_s $	5.24×10^{-4}	5.24×10^{-4}	5.24×10^{-4}
$ \Delta d_e $ (μm)	0.913	0.917	0.835
$ \Delta d_s $ (μm)	3.24	3.24	3.24

spectively. It can be seen that when θ approaches Brewster's angle ($\cong 57.99$ deg) of the silver-halide emulsion layer, both the phase difference ϕ_1 and its associated γ are almost equal to 0. Compromising between ϕ_1 and γ , $\theta = 59$ deg is chosen for our experiments.

The relations between ϕ_1 and α had been measured and depicted in Fig. 2. Here only the measured data for PFG-01 are rearranged and listed in the columns (α_1, α_2) and (ϕ_{11}, ϕ_{12}) of Table 5. The associated evaluated values of n and k are listed in the same table. From this table, it is obvious that the evaluated values of n and k are independent of (α_1, α_2) .



(a)



(b)

Fig. 3 Relation curves of (a) ϕ_1 versus α and (b) γ versus α for some different incident angles.

Table 5 The values of n and k for PFG-01 obtained at (α_1, α_2) .

(α_1, α_2)	(ϕ_{11}, ϕ_{12})	n	k
(20,30)	(4.508,2.835)	1.60921	0.000069
(30,40)	(2.835,1.949)	1.60926	0.000071
(40,50)	(1.949,1.372)	1.60922	0.000072
(50,60)	(1.372,0.943)	1.60925	0.000072
(60,70)	(0.943,0.595)	1.60923	0.00007

To avoid phase wrapping,²¹ it is necessary to let Ψ be smaller than π . So our experimental conditions are suitable for the emulsion layer and its substrate with thickness smaller than $\Lambda_{\text{eq}}/4(n-1)$ and $\Lambda_{\text{eq}}/4(n_s-1)$, respectively. Substituting $n \cong 1.67$ and $n \cong 1.52$ into $\Lambda_{\text{eq}}/4(n-1)$ and $\Lambda_{\text{eq}}/4(n_s-1)$, their measurable thicknesses are smaller than 14.93 and 19.23 mm, respectively.

5 Conclusions

An alternative method for measuring both the refractive indices and the thickness of the silver-halide emulsion layer and its substrate is presented by using the multiwavelength circularly polarized heterodyne interferometry. These optical parameters can be estimated with only one optical configuration. This method has many merits such as simple optical setup, easy operation, and rapid measurement. Its validity is demonstrated. It is suitable for the emulsion layer and its substrate with thicknesses smaller than 14.93 and 19.23 mm, respectively, in our experiments.

Acknowledgments

This study was supported in part by the National Science Council, Taiwan under contract NSC 92-2215-E-009-052.

References

1. P. Hariharan, *Optical Holography: Principles, Techniques, and Applications*, 2nd ed., Chap. 7, Cambridge University Press, Boston, MA (1996).
2. J. H. Chen, D. C. Su, and J. C. Su, "Shrinkage- and refractive-index shift-corrected volume holograms for optical interconnects," *Appl. Phys. Lett.* **81**, 1387–1389 (2002).
3. H. Kogelnik, "Coupled wave theory for thick hologram gratings," *Bell Syst. Tech. J.* **48**, 2909–2947 (1969).
4. See <http://www.aquila-instruments.com>.
5. C. Jung and B. K. Rhee, "Simultaneous determination of thickness and optical constants of polymer thin film by analyzing transmittance," *Appl. Opt.* **41**, 3861–3865 (2002).
6. X. Liu, P. Liang, W. Zhang, and Y. Tang, "Measuring the optical parameters of thin films by p -polarized laser beams," *Opt. Technol.* **30**, 85–89 (1998).
7. A. Belendez, T. Belendez, C. Neipp, and I. Pascual, "Determination of the refractive index and thickness of holographic silver halide materials by use of polarized reflectance," *Appl. Opt.* **41**, 6802–6807 (2002).
8. B. Smith, D. F. Clark, and C. Hamilton, "Characterization of planar antiresonant reflecting optical waveguide structures on silicon by an Abbe refractometer," *Opt. Lett.* **20**, 2084–2086 (1995).
9. M. V. Collados, I. Arias, A. Garcia, J. Atencia, and M. Quintanilla, "Silver halide sensitized gelatin process effects in holographic lenses recorded on Slavich PFG-01 plate," *Appl. Opt.* **42**, 805–810 (2003).
10. J. Rheims, J. Koser, and T. Wriedt, "Refractive-index measurements in the near-IR using an Abbe refractometer," *Meas. Sci. Technol.* **8**, 601–605 (1997).
11. C. Cali, M. Mosca, and G. Targia, "A simple apparatus for the determination of the optical constants and thickness of absorbing thin films," *Opt. Commun.* **191**, 295–298 (2001).
12. J. Jaglarz and M. Nowak, "Determination of optical constants and average thickness of thin films on thick substrates using angular distribution of intensity of reflected," *Thin Solid Films* **278**, 124–128 (1996).
13. T. Globus, G. Ganguly, and P. R. Cabarrocas, "Optical characterization of hydrogenated silicon thin films using interference technique," *J. Appl. Phys.* **88**, 1907–1915 (2000).
14. P. Yeh, *Optical Waves in Layered Media*, pp. 232–239, Wiley, New York (1991).
15. P. G. Charette, I. W. Hunter, and C. J. H. Brennan, "A complete high performance heterodyne interferometer displacement transducer for microactuator control," *Rev. Sci. Instrum.* **63**, 241–248 (1992).
16. R. Dandliker, Y. Salvade, and E. Zimmermann, "Distance measurement by multiple-wavelength interferometry," *J. Opt.* **29**, 105–114 (1998).
17. D. C. Su, M. H. Chiu, and C. D. Chen, "Simple two-frequency laser," *Precis. Eng.* **18**, 161–163 (1996).
18. A. Yariv and P. Yeh, *Optical Waves in Crystals*, p. 62, Wiley, New York (1983).
19. J. Y. Lin and D. C. Su, "A new type of optical heterodyne polarimeter," *Meas. Sci. Technol.* **14**, 55–58 (2003).
20. M. H. Chiu, J. Y. Lee, and D. C. Su, "Complex refractive-index measurement based on Fresnel's equations and the uses of heterodyne interferometry," *Appl. Opt.* **38**, 4047–4052 (1999).
21. P. K. Rastogi, *Optical Measurement Techniques and Applications*, p. 66, Artech House, Boston, MA (1997).



Cheng-Chih Hsu received his MS degree from the Institute of Applied Physics, Chung Yuan Christian University, Taiwan, in 1998, and is now working toward a PhD degree in optical metrology at the Institute of Electro-Optical Engineering of National Chiao Tung University. His current research activities are optical metrology and nondestructive testing.



Jiun-You Lin received his MS degree from the Institute of Electro-Optical Engineering of National Chiao Tung University, Taiwan, in 2000, and is now working toward a PhD degree in optical metrology at the Institute of Electro-Optical Engineering of National Chiao Tung University. His current research activities are optical metrology and measurement of optical constants of a chiral medium.



Kun-Huang Chen received his BS degree in physics from Chung Yuan Christian University, Taiwan, in 2000, and his PhD degree from the Institute of Electro-Optical Engineering of National Chiao Tung University, Taiwan, in 2004. He joined the faculty of Feng Chia University in 2004, where he is currently an assistant professor with the Department of Electrical Engineering. His current research activities are in optical metrology and optical sensors.



Der-Chin Su received his BS degree in physics from the National Taiwan Normal University in 1975 and his MS and PhD degrees in information processing from the Tokyo Institute of Technology in 1983 and 1986, respectively. He joined the faculty of the National Chiao Tung University in 1986, where he is currently a professor with the Institute of Electro-Optical Engineering. His current research interests are in optical testing and holography.